Proc., 5th World Congress of Biomechanics,
Held in Munich, D. Liepsch, ed.,
July 19-August 4, 2006, Medimond, Bologna
(ISBN 88-7587-271-6)

On Hyperelastic Constitutive Modeling of Annulus Fibrosus

F.C. Caner[1], Z.Y. Guo[2], B. Moran[3], Z.P. Bazant[3] and I. Carol[1]

[1] School of Civil Eng., Technical Univ. of Catalonia (UPC), Jordi Girona 1–3, 08034 Barcelona, Spain;[2] Depts. of Mechanical and Civil Eng., University of Glasgow, Glasgow, G12 8LT, Scotland; [3] Northwestern Univ., Dept. of Civil and Env. Eng., 2145 Sheridan Rd., Evanston IL 60208

Summary

In a recent paper, Peng et. al. [1] developed an anisotropic hyperelastic constitutive model for the human annulus fibrosus in which fiber–matrix interaction plays a crucial role in simulating experimental observations reported in the literature. Later, Guo et. al. [2] used fiber reinforced continuum mechanics theory to formulate a model in which the fiber–matrix interaction was simulated using only composite effect. It was shown in these studies that, the classical anisotropic hyperelastic constitutive models for soft tissue which do not account for this shear interaction cannot accurately simulate the test data on human annulus fibrosus. In this study, we show that the microplane model for soft tissue developed by Caner and Carol [5] can be adjusted for human annulus fibrosus and the resulting model can accurately simulate the experimental observations without accounting for fiber–matrix interaction. A comparison of results obtained from (i) a fiber–matrix parallel coupling model which does not account for the fiber–matrix interaction (ii) the same model but enriched with fiber–matrix interaction, and (iii) microplane model for soft tissue adapted to annulus fibrosus with 2 families of fiber distributions is presented.

Introduction

Recently, two papers, [1] and [2], have been submitted for publication in which the fiber–matrix interaction is shown to be indispensable for simulating mechanical behavior of annulus fibrosus by optimally fitting various experimental data from literature and contrasting the results obtained from the model with fiber–matrix interaction against those from the model without any such interaction. In this study, microplane model for soft tissue published in [5] is adapted for annulus fibrosus by incorporating two fiber families in accordance with the physiology of the lamellae. To be able to provide a fair comparison, the 1D fiber constitutive law is kept the same as in [1], except for the material parameters, which have to be readjusted because of the 3D angular fiber distribution employed in the microplane model. The constitutive model for the matrix is neo Hookean in this model as well [5,6]. In contrast, there is no explicit fiber–matrix interaction employed in microplane model for soft tissue. However, there is indeed interaction of distributed fibers provided automatically by construction of the model.

Hyperelastic fiber-matrix parallel coupling model

In this type of models, it is assumed that the strain energy function Ψ is a scalar function of the right Cauchy–Green deformation tensor, $\underline{\underline{C}} = \underline{\underline{F}}^T \cdot \underline{\underline{F}}$ where $\underline{\underline{F}}$ is the deformation gradient tensor, and the fiber direction in the reference configuration is given by $\underline{a}_0$ [3], i.e., $\Psi = \Psi(\underline{\underline{C}}, \underline{a}_0) = \Psi(I_1, I_2, I_3, I_4, I_5)$. The elastic response of a single layer of annulus fibrosus is assumed to comprise the resistance of the matrix, fibers and their interaction. Accordingly, the strain energy function Ψ can be divided into three parts given by $\Psi = \Psi^M + \Psi^F + \Psi^{FM}$ where Ψ^M is the strain energy contribution from the matrix, Ψ^F is the contribution from the fiber stretch and Ψ^{FM} is the strain energy caused by the fiber–matrix shear interaction. The invariants I_i are defined as $I_1 = \mathrm{tr}(\underline{\underline{C}})$; $I_2 = \{[\mathrm{tr}(\underline{\underline{C}})]^2 - \mathrm{tr}(\underline{\underline{C}}^2)\}/2$; $I_3 = \det \underline{\underline{C}}$; $I_4 = \underline{a}_0 \cdot \underline{\underline{C}} \cdot \underline{a}_0 = \lambda_F^2$; $I_5 = \underline{a}_0 \cdot \underline{\underline{C}}^2 \cdot \underline{a}_0$; λ_F=fiber stretch.

The energy Ψ^M stored in the matrix is assumed to be given by that for compressible neo Hookean material

$$\Psi^M = C_{10}(I_1^D - 3) + D_1^{-1}(J-1)^2 \tag{1}$$

where $J = I_3^{1/3}$ is the volume change and $I_1^D = J^{-2/3} I_1$ is the first invariant of the deviatoric right Cauchy– Green strain tensor, $C_{10} = \mu_0/2$ where μ_0 is the shear modulus and D_1^{-1} is the bulk modulus. The strain energy for fibers, Ψ^F is defined as

$$\Psi^F = \begin{cases} C_2(I_4-1)^2 + C_3(I_4-1)^4 & \text{if } I_4 > 1 \\ 0 & \text{if } I_4 \le 1 \end{cases} \tag{2}$$

where the second line in the equation above accounts for the fiber crimp under compression which leads to no contribution from the fiber, and the first line approximates the fiber contribution due to tensile fiber stretch.

To model the strain energy contributed by the fiber–matrix interaction, we consider a fiber direction in reference configuration given by $\underline{a}_0$ normal to a surface dS_0 which deforms into a surface dS with a surface normal given by $\underline{n}$, where the Nanson's formula [7] can be used to provide the relationship $\underline{n} dS = J \underline{a}_0 \cdot \underline{\underline{F}}^{-1} dS_0$. Thus,

$$\cos(\gamma) = \sqrt{I_3 [I_4 (I_5 - I_1 I_4 + I_2)]^{-1}} \tag{3}$$

that leads to a new invariant χ, defined as

$$\chi = \tan^2(\gamma) = \cos^{-2}(\gamma) - 1 = I_4 I_3^{-1}(I_5 - I_1 I_4 + I_2) - 1 \tag{4}$$

Now the strain energy function for fiber–matrix interaction can be defined as

$$\Psi^{FM} = \Psi^{FM}(I_4, \gamma) = f(I_4)\chi^2 \tag{5}$$

where χ is given by Eq.4 and $f(I_4)$ is given by

$$f(I_4) = \eta [1 + exp(-\beta(\lambda_F - \lambda_F^*))]^{-1} \tag{6}$$

where η is the largest $f(I_4)$ that can be achieved and $f(I_4)$ becomes $\eta/2$ at $\lambda_F = \lambda_F^*$; λ_F^* represents a transitional point in the fiber constitutive law and it must be calibrated to fit the experimental data along with η and β. It must be noted that when $\eta = 0$, the fiber–matrix interaction term disappears, making the model equivalent to a classical hyperelastic fiber–matrix parallel coupling model.

Now the constitutive law can be explicitly obtained in terms of 2nd Piola-Kirchoff stress tensor by taking the derivative of total strain energy Ψ with respect to the Green–Lagrangian strain tensor $\underline{\underline{E}} = (\underline{\underline{C}} - \underline{\underline{I}})/2$, i.e. $\underline{\underline{\Sigma}} = \partial \Psi / \partial \underline{\underline{E}} = 2 \partial \Psi / \partial \underline{\underline{C}}$. If two adjacent lamellae is to be modeled, then assuming that the two distinct fiber directions in the current configuration are given by $\underline{a}_1$ and $\underline{a}_2$, the Cauchy stress is given by

$$\begin{aligned} \underline{\underline{\sigma}} = {} & \frac{2}{J}\left[(I_2\Psi_{,2} + I_3\Psi_{,3})\underline{\underline{I}} + \Psi_{,1}\underline{\underline{B}} - I_3\Psi_{,2}\underline{\underline{B}}^{-1}\right] + \frac{1}{J}\left(I_{41}\Psi_{,41}\underline{a}_1 \otimes \underline{a}_1 + I_{42}\Psi_{,42}\underline{a}_2 \otimes \underline{a}_2\right) \\ & + \frac{1}{J}\left(I_{41}\Psi_{,51}\left(\underline{a}_1 \otimes \underline{\underline{B}} \cdot \underline{a}_1 + \underline{a}_1 \cdot \underline{\underline{B}} \otimes \underline{a}_1\right) + I_{42}\Psi_{,52}\left(\underline{a}_2 \otimes \underline{\underline{B}} \cdot \underline{a}_2 + \underline{a}_2 \cdot \underline{\underline{B}} \otimes \underline{a}_2\right)\right) \end{aligned} \tag{7}$$

where $I_{4\xi} = (\lambda_F^{\xi})^2$; $\Psi_{,i\xi} = \partial\Psi/\partial I_i^{\xi}$ and $\xi = 1,2$ are the indices of the fiber families; $i = 1,2,\ldots, 5$ are the indices of the invariants; $\underline{\underline{B}}$ is the left Cauchy Green tensor; $\Psi = \Psi^M + (\Psi_1^F + \Psi_2^F)/2 + (\Psi_1^{FM} + \Psi_2^{FM})/2$.

Microplane constitutive model for soft tissue

Isotropic incompressible neo-Hookean microplane model

The formulation for isotropic compressible neo Hookean microplane model was developed in [6] as part of a framework for hyperelastic microplane models and the anisotropic hyperelastic microplane model for blood vessel tissue was developed in [5]. In these formulations, the macroscopic free energy per unit volume, denoted $\rho_0\Psi$, is assumed to be integral of microplane free energies per unit area of a unit hemisphere Ψ_Ω, i.e.

$$\frac{2\pi R^3}{3}\rho_0\Psi = \int_\Omega \Psi_\Omega d\Omega \tag{8}$$

Here R = 1 is the radius of the unit hemisphere, Ω denotes the surface of the unit hemisphere, ρ_0 is the mass density, Ψ is the macroscopic free energy per unit mass per unit volume, Ψ_Ω is the microplane free energy per unit area given by

$$\Psi_\Omega(\lambda_D,\lambda_J) = \mu_0\left(\frac{\lambda_D^2}{2}+\frac{\lambda_D^{-3}}{2}-\frac{5}{6}\right)+\frac{1}{3}g(J) \tag{9}$$

In this equation, μ_0 is the material constant, λ_D is distortional stretch and J =det $\underline{\underline{F}}$ is the volume change with $\underline{\underline{F}} = \partial \underline{x}/\partial \underline{X}$ being the deformation gradient tensor and $g(J)$ is the volumetric energy function. The microplane stretch is defined as

$$\lambda_N = \lambda_D\lambda_J = \sqrt{\underline{N}\cdot\underline{\underline{C}}\cdot\underline{N}} \tag{10}$$

where $\lambda_J = J^{1/3}$ is the volumetric stretch, $\underline{N}$ is the microplane normal vector, $\underline{\underline{C}}$ is the right Cauchy-Green tensor. The volumetric energy function is given by

$$g(J) = \frac{\lambda_0}{2}\left(J+\frac{1}{J}-2\right) \tag{11}$$

It can be shown that substitution of Eqs. (9), (10) and (11) into Eq. (8) results in

$$\rho_0\Psi = \frac{\mu_0}{2}\left(I_1^D-3\right)+g(J) \tag{12}$$

where I_1^D is the first invariant of $\underline{\underline{C}}^D = J^{-2/3}\underline{\underline{C}}$.

Collagen fibers: Anisotropic microplane model

To account for many fiber directions using discrete representations, it is convenient to treat φ(N)as a probability density function that represents the fiber direction distribution in the material. For example, in [8] it is reported that under a microscopic study of arterial tissue, a directional distribution of densely packed collagen structures is observed. The probability density function corresponding to the distribution of orientation of cell nuclei (and thus that of the collagen fibers) in a human aortic media in 2-D reported in that study is given in Fig. 2. To facilitate the computations, the discrete data points are fitted with a convenient probability density function given by

$$\phi(\underline{N}) = \Phi(\theta) = c_1\, exp\left(c_2\theta^2\right) \tag{13}$$

where θ is the angle in radians measured from the circumferential direction. Thus, the proposed microplane constitutive law with a continuous representation of fiber directions in 3D can be expressed as

$$\underline{\underline{\Sigma}} = \frac{3}{2\pi}\int_\Omega\left(\left(\frac{\Sigma_D}{\lambda_D\lambda_J^2}+\phi(\underline{N})\Sigma_F\right)\underline{N}\otimes\underline{N}-\frac{\Sigma_D}{3}\lambda_D\underline{\underline{C}}^{-1}\right)d\Omega+\Sigma_J\lambda_J\underline{\underline{C}}^{-1} \tag{14}$$

Results and discussion

The predicted mechanical response from three different constitutive laws, namely fiber–matrix parallel coupling model without shear interaction between the fibers and matrix, fiber–matrix parallel coupling model with shear interaction between the fibers and matrix, and microplane model for annulus fibrosus, are demonstrated in Figs. 3 through 6. The responses by the fiber–matrix parallel coupling models with and without shear interaction between the fibers and matrix were obtained calibrating the constants C_{10}=0.034MPa, D_1=0.197MPa^{-1} for simulating the neo Hookean matrix behavior and the incompressibility; C_2=0.45MPa, C_3= 82.6MPa of the fiber law are determined from optimally fitting the data in Figs.3 and 4.

In Fig.3, the experimental data from several researchers in the form of engineering stress against engineering strain in the direction of loading of annulus fibrosus with inter-fiber angle of 60 facing the loading direction is plotted. The plot shows that the material properties of annulus fibrosus show significant differences;

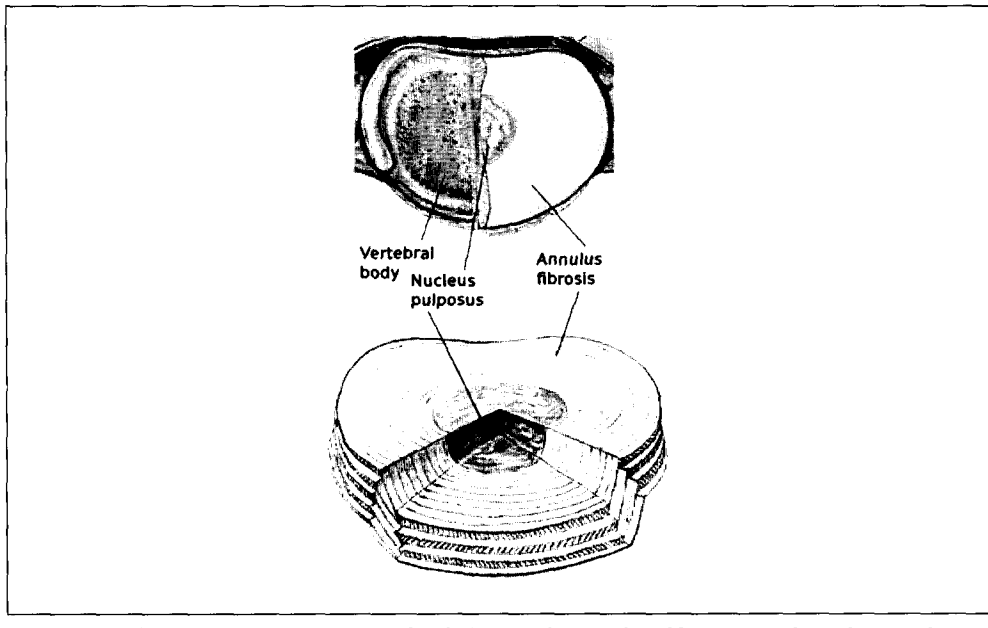

Figure 1: The top view of intervertebral disc with annulus fibrosus and nucleus pulposus, and oblique view of annulus fibrosus with nucleus pulposus. In the oblique view of annulus fibrosus, its lamellar structure and statistically dominant fiber directions that alternate from one lamella to other are depicted.

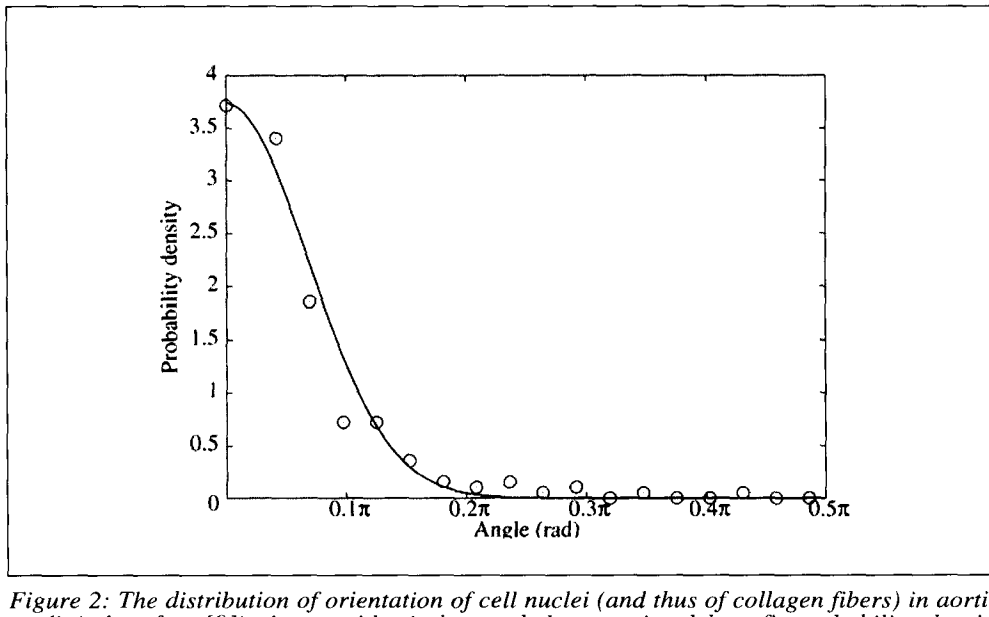

Figure 2: The distribution of orientation of cell nuclei (and thus of collagen fibers) in aortic media(taken from[8]) shown with circles, and the associated best fit probability density function.

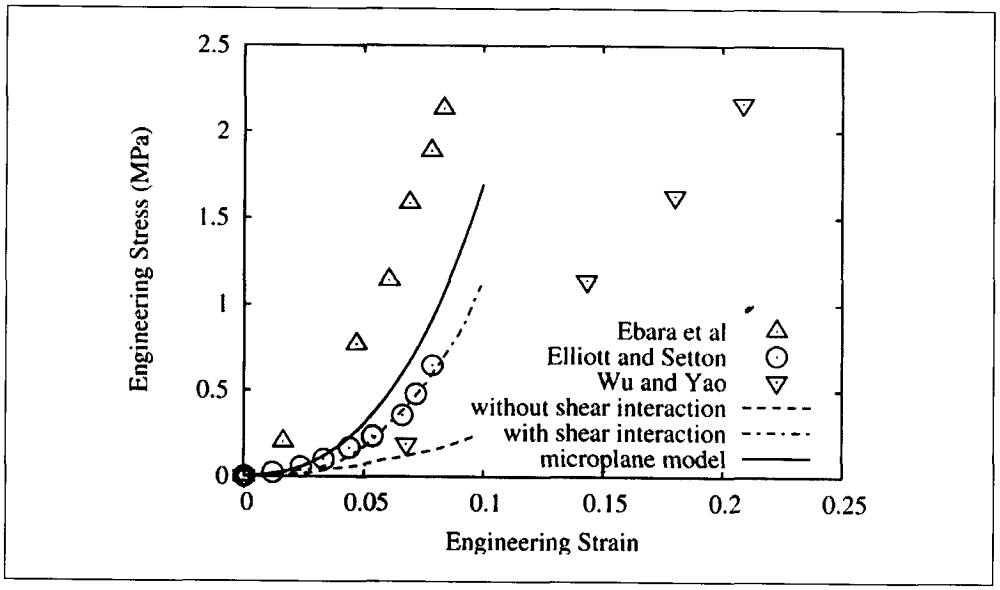

Figure 3: Tensile stress–strain behavior of multi–layer human anterior outer annulus fibrosus; inter–fiber angle facing the loading direction is 60 degrees.

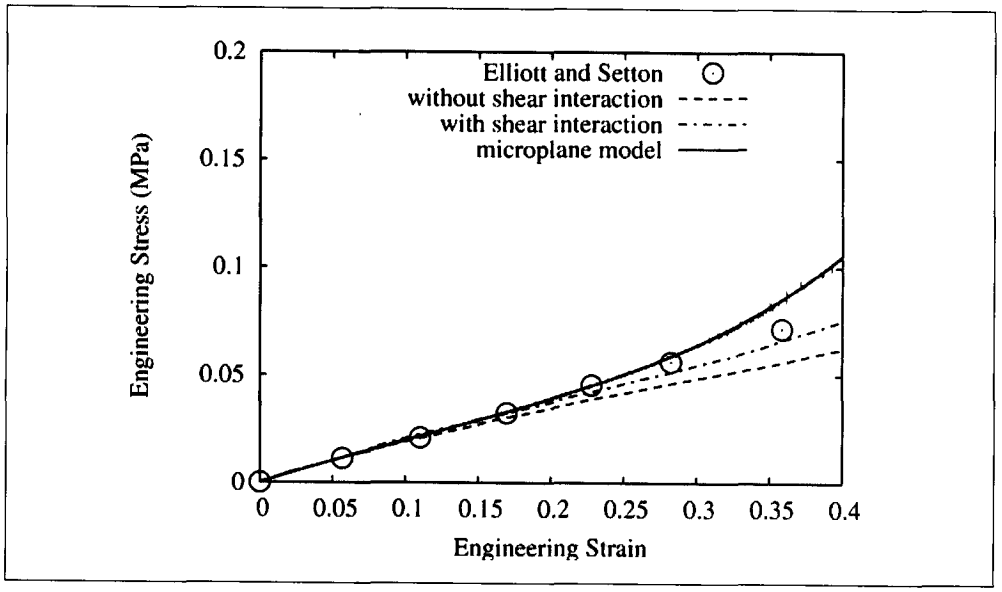

Figure 4: Tensile stress–strain behavior of multi–layer human anterior outer annulus fibrosus; inter–fiber angle facing the loading direction is 120 degrees.

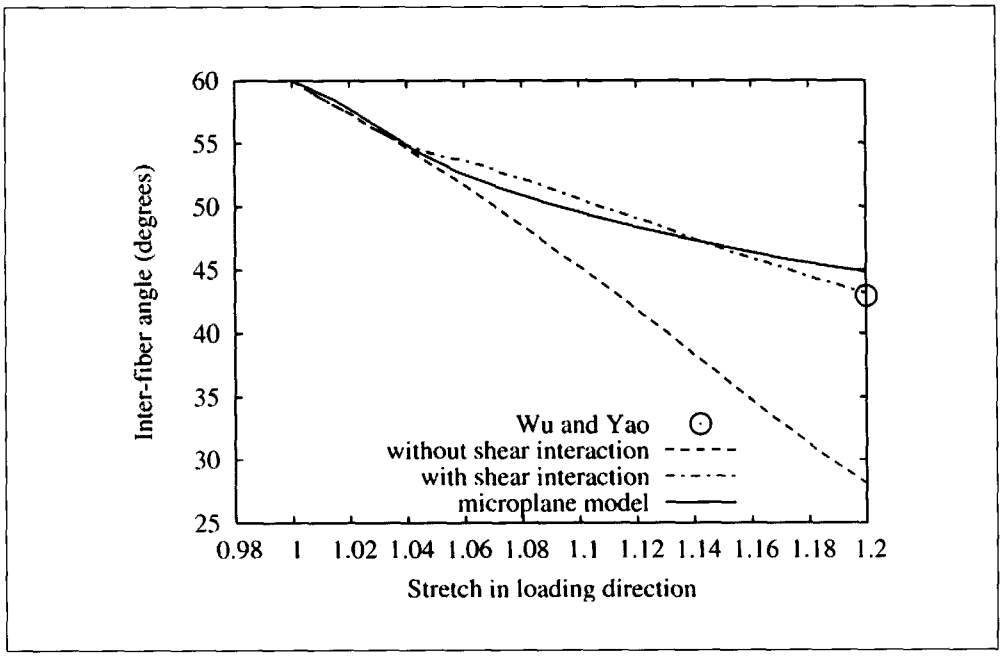

Figure 5: Inter–fiber angle change against stretch in the loading direction in multi–layer human anterior outer annulus fibrosus; inter–fiber angle facing the loading direction is 60 degrees.

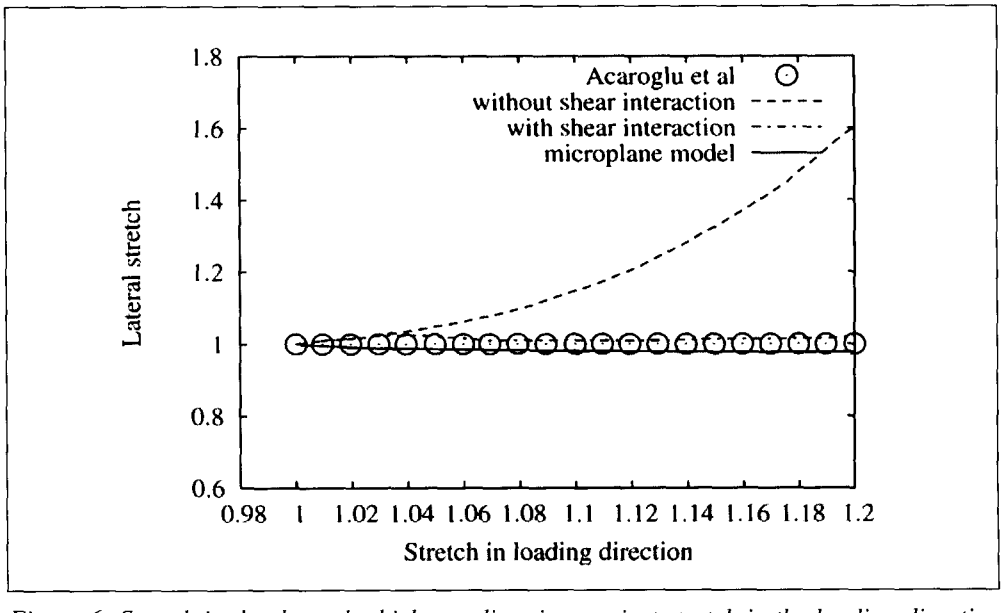

Figure 6: Stretch in the through–thickness direction against stretch in the loading direction in multi–layer human anterior outer annulus fibrosus; inter–fiber angle facing the loading direction is 60 degrees.

these differences are likely to be linked to factors such as age, lifestyle and diseases. In this study we chose to fit the one by Elliott and Setton [4], because they also provide equivalent data in the perpendicular direction, as shown in Fig.4. Fitting both of these data is required for any constitutive law. The parameters η =12MPa, β =125 and λ_F^* =1.02 of the parallel coupling model with fiber–matrix interaction are obtained by simultaneously fitting both of the test data appearing in Figs.3 and 4. All other test data are simulated with the material parameters being fixed.

The material parameters in microplane model, μ_0=0.068MPa, C_1=6.0MPa and C_2= 4000.0MPa as well as the parameters appearing in the fiber distribution law, c_1= 20.5 and c_2= -80.0 are obtained by simultaneous fitting of Figs.3 and 4. In Fig.5, which depicts variation of inter-fiber angle with stretch in the loading direction, microplane model performs very well despite the fact that it does not have the explicit formulation for interaction. The parallel coupling model with interaction also performs very well, but the performance of that without the interaction might not be considered acceptable.

In Fig. 6 in which the lateral through thickness stretch is plotted against loading direction stretch, microplane model performs as good as parallel coupling model with shear interaction; that without the interaction performs probably beyond the acceptable limits.

Conclusions

Three models for the mechanical behavior of annulus fibrosus, namely fiber–matrix parallel coupling model, fiber–matrix parallel coupling model with fiber–matrix shear interaction and microplane model for soft tissue adjusted for the annulus fibrosus, are compared against experimental data available in the literature and against each other. The microplane model for soft tissue does not contain any explicit formulation for shear interaction. However the construction of the model allows such an interaction to take place between the fibers at material point level in contrast to the finite element level as in the case of parallel coupling model without shear interaction. Physically this is equivalent to a combined inter-lamellar interaction of distributed fibers in different lamellae as well as interaction between the distributed fibers in the same lamella. We note that intensity of the shear interaction between the fibers can be adjusted by adjusting the spread in the distribution while keeping the total amount of fibers constant. Another aspect of microplane model is that the anisotropic effect of the fibers is homogenized due to the volume averaging in the formulation of the model [5,6]. The consequence of averaging is that the anisotropy causing singularities can be represented conveniently in the model. For example, a discrete fiber direction will appear in the microplane model as a Dirac delta function. Thus, the volume averaging inherent in the microplane model admits the interpretation that the microplane stresses are those that belong to a lower scale than the continuum scale, although it is rather difficult to identify this scale precisely.

It is clear that the parallel coupling model performs very well in all the simulations, and it is equally clear that without shear interaction, this model cannot be reliably used for the mechanics of outer annulus fibrosus. Microplane model, on the other hand, performs very well despite not having any explicit fiber-matrix interaction.

The behavior of microplane model can be adjusted by adjusting the spread in the fiber distribution keeping the area under the distribution constant (Fig.2). For example, when the spread drops too much, the fits in Figs.5 and 6 are affected in such a way that the response approaches that predicted by the parallel coupling model without shear interaction. Thus, in microplane model, the angular fiber distribution competes against an explicit fiber–matrix interaction. If experimental data were available indicating a common incidence of a particular angular fiber distribution, the parameters of the distribution could no longer be used in data fitting, and to be able to fit the test data, an explicit fiber–matrix or fiber–fiber interaction would have to be introduced.

References

[1] PENG, X. Q., GUO, Z. Y., AND MORAN, B., 2006. "An anisotropic hyperelastic constitutive model with fiber–matrix interaction for the human annulus fibrosus". J. of Applied Mechanics, in press.
[2] GUO, Z. Y., PENG, X. Q., AND MORAN, B., 2006. "A composites–based hyperelastic constitutive model for soft tissue with application to the human annulus fibrosus". J. of the Mechanics and Physics of Solids, in press.
[3] SPENCER, A. J. M., 1984. Continuum theory of the mechanics of fiber-reinforced composites. Springer, New York.
[4] ELLIOTT, D. M., AND SETTON, L.A., 2001. "Anisotropic and inhomogeneous tensile behavior of the human annulus fibrosus: Experiments measurement and material model predictions". J. of Biomechanical Engineering, 123, pp. 256–263.
[5] CANER, F. C., AND CAROL, I., 2006. "Microplane constitutive model and computational framework for blood vessel tissue". J. of Biomechanical Engineering – Transactions of the ASME, 128(3),pp. 419– 427.
[6] CAROL, I., JIRÁSEK, M., AND BAŽANT, Z. P., 2004. "A framework for microplane models at large strain, with application to hyperelasticity". Int. J. of Solids and Structures, 41(2), pp. 511–557.
[7] MALVERN, L. E., 1969. Introduction to the Mechanics of Continuous Medium. Prentice–Hall, Englewood Cliffs, New Jersey.
[8] HOLZAPFEL, G. A., 2003. "Structural and numerical models for the (visco) elastic response of arterial walls and residual stresses". In Biomechanics of soft tissue in cardiovascular systems, G.A. Holzapfel and R. W. Ogden, eds. Springer Wien New York, pp. 109–184.